



# Performance analysis of full-duplex decode-and-forward two-way relay networks with transceiver impairments

Ba Cao Nguyen<sup>1,2</sup> · Xuan Nam Tran<sup>1</sup> · Dinh Tan Tran<sup>2</sup>

Received: 21 August 2019 / Accepted: 6 July 2021 / Published online: 3 August 2021  
© Institut Mines- and Springer Nature Switzerland AG 2021

## Abstract

In this paper, we analyze the performance of an in-band full-duplex (IBFD) decode-and-forward (DF) two-way relay (TWR) system whose two terminal nodes exchange information via a relay node over the same frequency and time slot. Unlike the previous works on full-duplex two-way relay systems, we investigate the system performance under the impacts of both hardware impairments and imperfect self-interference cancellation (SIC) at all full-duplex nodes. Specifically, we derive the exact expression of outage probability based on the signal to interference plus noise and distortion ratio (SINDR), thereby determine the throughput and the symbol error probability (SEP) of the considered system. The numerical results show a strong impact of transceiver impairments on the system performance, making it saturate at even a low level of residual self-interference. In order to tackle with the impact of hardware impairments, we derive an optimal power allocation factor for the relay node to minimize the outage performance. Finally, the numerical results are validated by Monte Carlo simulations.

**Keywords** Full-duplex two-way relay · Self-interference cancellation · Decode-and-forward · Outage probability · Symbol error probability · Hardware impairments

## 1 Introduction

With the increasing demand for high-rate data transmission, the wireless systems need to use more bandwidth for their transmission. Meanwhile, the number of wireless devices is expected to increase dramatically in the era of the fourth industrial evolution with every thing connected to the Internet. The radio frequency is becoming scarce due to limited radio spectrum. Therefore, transmission technologies with high spectral efficiency are expected to develop for future deployment. Recent researches in the literature showed a great interest in the in-band full-duplex (IBFD) and two-way relay (TWR) communications.

While the IBFD systems can attain a double spectrum efficiency thanks to the simultaneous use of the same spectral bandwidth for both transmitter and receiver [1, 2], the TWR systems increase its spectral efficiency by letting the two end nodes simultaneously transmit and receive at the same time slot. The combination of the TWR and IBFD communications provides an IBFD TWR system that enables high-rate data transmission and improves spectral efficiency [3–6]. However, this system becomes more vulnerable to the residual self-interference (RSI) at all nodes, i.e. the two terminal nodes and the relay node, due to imperfect self-interference cancellation (SIC) [7–10].

Previous studies on the IBFD TWR systems paid significant attention on analyzing their performance under the case of imperfect SIC. In [3], the outage probability (OP) of the IBFD TWR system with the amplify-and-forward (AF) protocol is determined for the case of perfect and imperfect channel state information (CSI). The paper showed that the OP of the system soon exhibits an error floor at the high signal to noise ratio (SNR) regime due to the imperfect CSI. In [4], the performance of the IBFD TWR system is analyzed and optimized for the case with multiple relays. The authors derived the exact OP, bit error rate (BER) and ergodic capacity of the system. The paper also demonstrated that the IBFD TWR system achieved

---

✉ Xuan Nam Tran  
namtx@mta.edu.vn

Ba Cao Nguyen  
bacao.sqtt@gmail.com

Dinh Tan Tran  
trdinhtan@gmail.com

<sup>1</sup> Le Quy Don Technical University, Hanoi, Vietnam

<sup>2</sup> Telecommunications University, Khanh Hoa, Vietnam

higher efficiency and better performance than the half-duplex (HD) TWR one when the RSI is sufficiently small. In [11], the authors proposed a multi-pair IBFD AF-TWR system which used one shared-antenna at each terminal node and  $M$  shared-antennas at the relay node. An optimal power allocation scheme was also proposed to improve the system performance in the case of none power-scaling. In [12], the OP of the IBFD multi-user AF-TWR system was analyzed. The paper studied the impact of the RSI incurred by the IBFD mode on the system performance and showed the full duplex (FD) mode could achieve the desired performance within the low RSI regime. However, when the RSI increased, the performance gain of the FD mode was lower than that of the HD mode. In [13], the achievable rate of the IBFD AF-TWR system with joint relay and antenna selection was considered. The impacts of the RSI and transmit power on the system performance were also studied. The achievable rate of this system was shown to increase quickly in the low SNR and then reach a saturated level in the high SNR regime.

Besides the AF protocol, the decode-and-forward (DF) was also proposed to use in the IBFD TWR systems. In [5] and [6], the OP was used as the performance criterion to evaluate the performance of the IBFD DF-TWR system. The authors derived the OP expression for seven different cases corresponding to the power allocation factor at the relay node. The paper also investigated the OP for both symmetrical and asymmetrical systems. The OP of the IBFD DF-TWR system was analyzed for the case with both imperfect CSI and imperfect SIC in [14]. The paper also considered the impact of imperfect CSI on power allocation and optimal relay placement. The work in [15] considered a multi-user IBFD DF-TWR system and proposed a max-min scheduling scheme to optimize the system outage performance. It was shown that in the case of full CSI, the system outage performance could be improved by the max-min scheduling scheme. In [16], the authors evaluated the spectrum efficiency of the IBFD DF-TWR system when using the sum rate as a function of the distance between the terminal and the relay node. In [17], the authors considered the secrecy performance of the IBFD DF-TWR system with the optimal relay selection. It was shown that the secrecy performance was significantly affected by the number of relays, the average signal to noise ratio (SNR) of eavesdropper links, and the RSI. The work [18] proposed a self-interference management scheme based on the cooperative communications for the multiuser IBFD DF-TWR system. It is noted that although the performance of the IBFD TWR system was extensively studied, most previous works only focused on its OP leaving other performance parameters such as the error rate and the system throughput opened for further investigation.

Given the assumption that the system hardware is not ideal due to different factors, such as manufacturing imperfection, phase oscillator noises, and I/Q imbalance, the performance of the IBFD TWR systems was also studied in previous works. In [19], the imperfect high power amplifier (HPA), imperfect SIC, and modulation imbalance at the relay node were considered for the IBFD AF one-way relay system. It was demonstrated that the received SNR at the relay node did not affect the input back-off (IBO) optimization and the bit error rate (BER) could be minimized by the optimal IBO when the channel between the relay and the destination node is flat fading. In [20] and [21], the authors studied the impact of hardware impairments at both transmitter and receiver in the IBFD one-way relay system using both AF and DF protocols. The paper showed a significant performance degradation by the hardware impairments, especially at high transmission rate. The work in [22] investigated the performance of a switch-and-examine relay system with post-selection scheduling under the impact of hardware impairment in the shadowed-Rician channel. The problems of both hardware impairments and imperfect channel estimation in the one-way relay and TWR AF systems were analyzed in [23]. Both the systems were shown to suffer from an outage floor but that in the one-way system was lower than in the TWR system.

Recently, the joint and cross impacts of hardware impairments (HI) and RSI on the performance of IBFD relay systems have also been investigated [10, 24–30]. However, these works focused on the IBFD one-way relay (OWR) systems [25–30] or IBFD TWR system with AF protocol [10, 24]. Due to the difficulty in solving mathematical equations, the system performance of the IBFD TWR system using DF protocol with HI and RSI was not analyzed. This motivates us to consider the IBFD DF-TWR system under the simultaneous impacts of hardware impairments and imperfect SIC at all nodes. Specifically, we aim to analyze its performances in terms of the outage probability, throughput, and symbol error probability (SEP) and compare them with those of the ideal hardware system in [5, 6]. Against the previous works, the contributions of our paper can be summarized as follows:

- We first determine the exact expression of the signal to interference plus noise and distortion ratio (SINDR) and use it to derive a new closed-form expression for the OP of the system as a function of the power allocation factor at the relay node. Unlike the previous works in [5, 6, 14, 15], which examined the OP based on the SIC capabilities of only the relay, we consider them at all FD nodes in our analysis. On the other hand, we also determine the OP according to the average SNR of the system to explore the outage behaviour of both the

ideal hardware and the hardware impairment systems. The system throughput and SER are also analyzed to determine the impact of hardware impairments and RSI on the system performance.

- Moreover, we analyze the system performance under the impacts of both hardware impairments and the RSI. The level of the RSI is then varied with the transmit power of the FD nodes to have an insight into the impact of the RSI at the high SNR regime. Based on this observation, we derive an optimal power allocation factor for the relay node to minimize the OP and SEP.

The rest of the paper is organized as follows. The system model and its related assumptions are described in Section 2. Section 3 presents the performance analysis of the system in terms of the outage probability, throughput, and symbol error probability. The proposed optimal power allocation factor is presented in Section 4. Numerical results and discussions are given in Section 5. Finally, Section 6 draws the conclusion of the paper.

## 2 System model

In order to describe the system model of a IBFD DF-TWR network with hardware impairments, we first begin with a simple point-to-point communication system which has two end nodes, each equipped with an antenna for both transmission and reception. In the case of ideal hardware, the received signal at one node is given by

$$y = hx + z, \tag{1}$$

where  $x$  is the transmitted signal,  $h$  is the fading coefficient of the link between the two nodes, and  $z$  is the additive white Gaussian noise (AWGN) with zero-mean and variance of  $\sigma^2$ , i.e.  $z \sim \mathcal{CN}(0, \sigma^2)$  at the receiver.

In the case of hardware impairments, the received signal with the same above conditions is given by

$$y = h(x + \eta_t) + \eta_r + z, \tag{2}$$

where  $\eta_t$  and  $\eta_r$  are the distortion noises due to the impairments at the transmitter and the receiver, respectively,  $\eta_t \sim \mathcal{CN}(0, k_t^2 P)$  and  $\eta_r \sim \mathcal{CN}(0, k_r^2 P|h|^2)$ ; The two design parameters  $k_t$  and  $k_r$  represent the impairment level at the transmitter and the receiver, respectively. For a given channel  $h$ , the aggregate distortion at the receiver is given by

$$\mathbb{E}_{\eta_t, \eta_r} \{|h\eta_t + \eta_r|^2\} = P|h|^2(k_t^2 + k_r^2), \tag{3}$$

where  $\mathbb{E}\{\cdot\}$  denotes the expectation operator. The aggregate distortion at the receiver depends on the average signal power  $P = \mathbb{E}\{|x|^2\}$ , the instantaneous channel gain  $|h|^2$ , and the design parameters  $k_t^2$  and  $k_r^2$ . Let  $k^2 = k_t^2 + k_r^2$  then the aggregate distortion at the receiver becomes

$$\mathbb{E}_{\eta_t, \eta_r} \{|h\eta_t + \eta_r|^2\} = P|h|^2 k^2, \tag{4}$$

where  $k$  is the aggregate impairment level which accounts for that from the transmitter hardware  $k_t$  and the receiver hardware  $k_r$ . Since  $k$  depends on the transmit power, it may vary during practical operation. However, for simplicity, we assume that  $k$  is constant, which is appropriate for a certain transmitter power level.

Using Eq. 4, the received signal in Eq. 2 is rewritten as

$$y = h(x + \eta) + z, \tag{5}$$

where  $\eta$  represents the aggregate hardware impairment at both transmitter and receiver with  $\eta \sim \mathcal{CN}(0, k^2 P)$ . Under these assumptions, we can establish the system model for the considered IBFD DF-TWR relay network with hardware impairments as illustrated in Fig. 1.

During the multiple access (MA) phase, the two end nodes  $S_1$  and  $S_2$  exchange data with each other via a relay

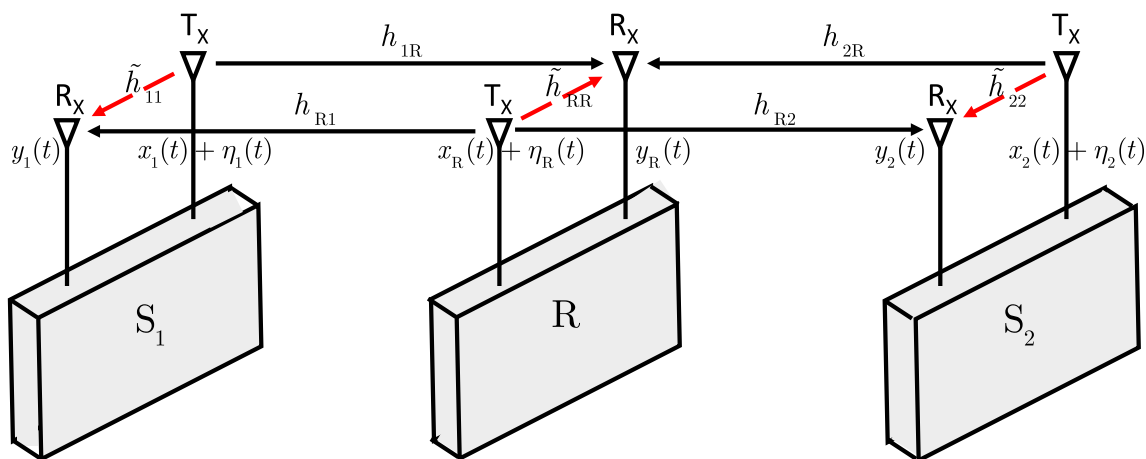


Fig. 1 System model of a IBFD DF-TWR network with transceiver impairments

node R and the received signal at the relay node at a time slot  $t$  is given by

$$y_R(t) = h_{1R}\tilde{x}_1(t) + h_{2R}\tilde{x}_2(t) + \tilde{h}_{RR}\tilde{x}_R(t) + z_R(t), \quad (6)$$

where  $\tilde{x}_1(t) \triangleq x_1(t) + \eta_1(t)$ ;  $\tilde{x}_2(t) \triangleq x_2(t) + \eta_2(t)$ ;  $\tilde{x}_R(t) \triangleq x_R(t) + \eta_R(t)$ , with  $x_1(t)$ ,  $x_2(t)$ , and  $x_R(t)$  are the desired signals, while  $\tilde{x}_1(t)$ ,  $\tilde{x}_2(t)$ , and  $\tilde{x}_R(t)$  are the actual signals from  $S_1$ ,  $S_2$ , and R, respectively;  $\eta_1(t)$ ,  $\eta_2(t)$ , and  $\eta_R(t)$  are the distortions caused by the transmitter and the receiver of nodes  $S_1$ ,  $S_2$ , and R with  $\eta_1 \sim \mathcal{CN}(0, k_1^2 P_1)$ ,  $\eta_2 \sim \mathcal{CN}(0, k_2^2 P_2)$ , and  $\eta_R \sim \mathcal{CN}(0, k_R^2 P_R)$ ;  $P_i$  is the transmit power and  $k_i$  indicates the impairment level of each node, where  $i = 1, 2, R$  corresponding to node  $S_1$ ,  $S_2$ , and R;  $h_{1R}$ ,  $h_{2R}$ , and  $\tilde{h}_{RR}$  represent the fading coefficients of the channels from  $S_1$ ,  $S_2$  to R and from the transmitting antenna to the receiving antenna of R;  $z_R \sim \mathcal{CN}(0, \sigma_R^2)$  denotes the AWGN at the relay. Note that when  $k_1 = k_2 = k_R = 0$ , the considered system becomes an ideal-hardware one.

During the broadcast (BC) phase, at the same time slot  $t$ , the relay node R transmits the encoded signal comprised of the received signals from the MA phase to  $S_1$ ,  $S_2$ . The received signals at  $S_1$ ,  $S_2$  are given respectively by

$$y_1(t) = h_{R1}\tilde{x}_R(t) + \tilde{h}_{11}\tilde{x}_1(t) + z_1(t), \quad (7)$$

$$y_2(t) = h_{R2}\tilde{x}_R(t) + \tilde{h}_{22}\tilde{x}_2(t) + z_2(t), \quad (8)$$

where  $h_{R1}$ ,  $h_{R2}$ ,  $\tilde{h}_{11}$ ,  $\tilde{h}_{22}$  are the fading coefficients of the links from R to  $S_1$ , from R to  $S_2$  and from transmitting antenna to receiving antenna of  $S_1$ ,  $S_2$ , respectively. It is noted that two channel models are often applied for IBFD TWR systems, i.e. reciprocal channels and non-reciprocal channels. The case of reciprocal channels is used when the overall user-to-relay and relay-to-user transmission time falls within a coherence interval of the channel and the pair of antennas are placed sufficiently close distance. Meanwhile, the case of non-reciprocal channels is appropriate when the pair of antennas are implemented far apart each other for transmission and reception [31]. In this paper, we assume that the distance between transmit and receive antennas of a node is sufficiently close; thus, the channels are reciprocal. This assumption are widely used in the literature such as [4, 6, 14, 31, 32]. In other word, we have  $|h_{R2}|^2 = |h_{2R}|^2$ ,  $|h_{R1}|^2 = |h_{1R}|^2$ ;  $z_i \sim \mathcal{CN}(0, N_i)$ ,  $i = 1, 2$  is AWGN.

The transmitted signal  $\tilde{x}_R(t)$  at R consists of two signals  $\tilde{x}_1(t)$  and  $\tilde{x}_2(t)$  as follows:  $\tilde{x}_R(t) = \tilde{x}_1(t) + \tilde{x}_2(t) + \eta_R(t)$ . In fact,  $\tilde{x}_R(t)$  contains the two previous received signals  $x_1(t - 1)$  and  $x_2(t - 1)$  with different power allocation levels for re-encoding such that  $\mathbb{E}\{|\tilde{x}_1(t)|^2\} = (1 - \lambda)P_R$ ,  $\mathbb{E}\{|\tilde{x}_2(t)|^2\} = \lambda P_R$ , where  $\lambda \in (0, 1)$ . Using a suitable network coding technique such as in [4],  $S_1$  and  $S_2$  can fully

extract the intended signal transmitted to them from  $\tilde{x}_R(t)$  and we have

$$y_1(t) = h_{R1}[\tilde{x}_2(t) + \eta_R(t)] + \tilde{h}_{11}\tilde{x}_1(t) + z_1(t), \quad (9)$$

$$y_2(t) = h_{R2}[\tilde{x}_1(t) + \eta_R(t)] + \tilde{h}_{22}\tilde{x}_2(t) + z_2(t). \quad (10)$$

Assume that effective SIC techniques are used in all three nodes so that the RSI after SIC, denoted by  $I_i$ , can be modeled by a complex Gaussian distributed random variable [3, 4, 6, 16, 32–34] with zero-mean and variance  $\sigma_{RSI_i}^2 = \tilde{\Omega}_i P_i$ , where  $\tilde{\Omega}_i$  denotes the SIC capability of node  $i$ ,  $i = 1, 2, R$ . Equations 6, 9, and 10 then can be rewritten as

$$y_R(t) = h_{1R}\tilde{x}_1(t) + h_{2R}\tilde{x}_2(t) + I_R + z_R(t), \quad (11)$$

$$y_1(t) = h_{R1}[\tilde{x}_2(t) + \eta_R(t)] + I_1 + z_1(t), \quad (12)$$

$$y_2(t) = h_{R2}[\tilde{x}_1(t) + \eta_R(t)] + I_2 + z_2(t). \quad (13)$$

From Eqs. 11, 12, 13, the SINDRs of the IBFD DF-TWR system are given by

$$\gamma_{S1R} = \frac{\rho_1 P_1}{\sigma_R^2 + \sigma_{RSIR}^2 + \rho_1 k_1^2 P_1 + \rho_2 k_2^2 P_2}, \quad (14)$$

$$\gamma_{S2R} = \frac{\rho_2 P_2}{\sigma_R^2 + \sigma_{RSIR}^2 + \rho_1 k_1^2 P_1 + \rho_2 k_2^2 P_2}, \quad (15)$$

$$\gamma_{RS1} = \frac{\rho_1 \lambda P_R}{\sigma_1^2 + \sigma_{RSI1}^2 + \rho_1 k_R^2 P_R}, \quad (16)$$

$$\gamma_{RS2} = \frac{\rho_2 (1-\lambda) P_R}{\sigma_2^2 + \sigma_{RSI2}^2 + \rho_2 k_R^2 P_R}, \quad (17)$$

$$\gamma_{\text{sum}} = \frac{\rho_1 P_1 + \rho_2 P_2}{\sigma_R^2 + \sigma_{RSIR}^2 + \rho_1 k_1^2 P_1 + \rho_2 k_2^2 P_2}, \quad (18)$$

where  $\rho_1 = |h_1|^2 = |h_{R1}|^2 = |h_{1R}|^2$ ;  $\rho_2 = |h_2|^2 = |h_{R2}|^2 = |h_{2R}|^2$ ;  $\gamma_{S1R}$ ,  $\gamma_{S2R}$ ,  $\gamma_{RS1}$ ,  $\gamma_{RS2}$  represent the SINDR of the communication links from  $S_1$  and  $S_2$  to R, from R to  $S_1$  and  $S_2$ , respectively;  $\gamma_{\text{sum}}$  denotes that of the sum signal at the relay node.

### 3 Performance analysis

#### 3.1 Outage probability analysis

In this section, we analyze the performance of the IBFD DF-TWR system and derive the exact OP expression for different cases of power allocation factors. The OP is defined as the achievable rate of any communication links which is less than the minimum data rate that the system must achieve. Assume that the minimum required data rate from  $S_1$  to R and from R to  $S_2$  is  $\mathcal{R}_1$ , from  $S_2$  to R and from R to  $S_1$  is  $\mathcal{R}_2$ . OP of a random link between  $S_1$ , R,  $S_2$  can be defined as follows:

$$\mathcal{P}_{\text{out}} = \Pr\{C_j < \mathcal{R}_j\}, \quad (19)$$

where  $C_j = \log_2(1 + \gamma_j)$  and  $\gamma_j, \mathcal{R}_j$  are the SINDR and the minimum required data rate of link  $j, j = 1, 2$ , respectively. Therefore, the OP occurs when

$$\log_2(1 + \gamma_{S_1R}) < \mathcal{R}_1 \text{ or } \log_2(1 + \gamma_{RS_2}) < \mathcal{R}_1, \tag{20}$$

$$\log_2(1 + \gamma_{S_2R}) < \mathcal{R}_2 \text{ or } \log_2(1 + \gamma_{RS_1}) < \mathcal{R}_2, \tag{21}$$

$$\log_2(1 + \gamma_{\text{sum}}) < \mathcal{R}_1 + \mathcal{R}_2. \tag{22}$$

Equivalently, we have

$$\gamma_{S_1R} < 2^{\mathcal{R}_1} - 1 \text{ or } \gamma_{RS_2} < 2^{\mathcal{R}_1} - 1, \tag{23}$$

$$\gamma_{S_2R} < 2^{\mathcal{R}_2} - 1 \text{ or } \gamma_{RS_1} < 2^{\mathcal{R}_2} - 1, \tag{24}$$

$$\gamma_{\text{sum}} < 2^{\mathcal{R}_1 + \mathcal{R}_2} - 1. \tag{25}$$

Let  $x = 2^{\mathcal{R}_1} - 1, y = 2^{\mathcal{R}_2} - 1$ , it then follows that  $2^{\mathcal{R}_1 + \mathcal{R}_2} - 1 = x + y + xy$ , and we can determine the OP as follows:

$$\mathcal{P}_{\text{out}} = \Pr\{\mathcal{A} \cup \mathcal{B} \cup \mathcal{C}\}, \tag{26}$$

where the events  $\mathcal{A}, \mathcal{B}, \mathcal{C}$  are defined in the following expressions:

$$\begin{aligned} \mathcal{A} &= (\gamma_{S_1R} < x) \cup (\gamma_{RS_1} < y), \\ \mathcal{B} &= (\gamma_{S_2R} < y) \cup (\gamma_{RS_2} < x), \\ \mathcal{C} &= (\gamma_{\text{sum}} < z), \end{aligned} \tag{27}$$

with  $z = x + y + xy$ .

Under the Rayleigh fading channel, the CDF and PDF of the channel gains  $\rho_l = |h_l|^2, l = 1 \div 2$  are given, respectively, by

$$F_{\rho_l}(x) = 1 - e^{-\frac{x}{\Omega_l}}, f_{\rho_l}(x) = \frac{1}{\Omega_l} e^{-\frac{x}{\Omega_l}}, x \geq 0, \tag{28}$$

where  $\Omega_l = \mathbb{E}\{|h_l|^2\}$ .

We assume further that the relay node knows the global CSI to decode successfully the received signal and the two terminal nodes know the partial CSI to subtract the transmitted signals.

**Theorem 1** *Under the Rayleigh fading channel and hardware impairments, we can determine the accurate OP expression for the following seven cases:*

$$\mathcal{P}_{\text{out}} = \begin{cases} 1 - Q_2 Q_3, & \text{case 1,} \\ 1 - Q_2 Q_3 Q_5, & \text{case 2,} \\ 1 - Q_1 Q_3 Q_5, & \text{case 3,} \\ 1 - Q_2 Q_4 Q_5, & \text{case 4,} \\ 1 - Q_2 Q_4, & \text{case 5,} \\ 1 - Q_1 Q_4 Q_5, & \text{case 6,} \\ 1 - Q_1 Q_4, & \text{case 7,} \end{cases} \tag{29}$$

where

$$Q_1 = \frac{a_{12}}{a_{12} + b_{12}} \exp\left(-\frac{xt_R}{a_{12}}\right), \tag{30}$$

$$Q_2 = \exp\left(-\frac{yt_1}{c_{12}}\right) \left[1 - \frac{b_{12}}{a_{12} + b_{12}} \exp\left(\frac{xt_R c_{12} - yt_1 a_{12}}{b_{12} c_{12}}\right)\right], \tag{31}$$

$$Q_3 = \frac{a_{34}}{a_{34} + b_{34}} \exp\left(-\frac{yt_R}{a_{34}}\right), \tag{32}$$

$$Q_4 = \exp\left(-\frac{xt_2}{c_{34}}\right) \left[1 - \frac{b_{34}}{a_{34} + b_{34}} \exp\left(\frac{yt_R c_{34} - xt_2 a_{34}}{b_{34} c_{34}}\right)\right], \tag{33}$$

$$Q_5 = \begin{cases} \frac{a_5}{a_5 - b_5} \exp\left(-\frac{zt_R}{a_5}\right), & \begin{cases} 1 - k_1^2 z \leq 0, \\ 1 - k_2^2 z > 0, \end{cases} \\ \frac{b_5}{b_5 - a_5} \exp\left(-\frac{zt_R}{b_5}\right), & \begin{cases} 1 - k_1^2 z > 0, \\ 1 - k_2^2 z \leq 0, \end{cases} \\ \frac{a_5}{a_5 - b_5} \exp\left(-\frac{zt_R}{a_5}\right) + \frac{b_5}{b_5 - a_5} \exp\left(-\frac{zt_R}{b_5}\right), & \begin{cases} 1 - k_1^2 z > 0 \\ 1 - k_2^2 z > 0, \\ a_5 \neq b_5, \end{cases} \\ \left(1 + \frac{zt_R}{a_5}\right) \exp\left(-\frac{zt_R}{a_5}\right), & \begin{cases} 1 - k_1^2 z > 0, \\ 1 - k_2^2 z > 0, \\ a_5 = b_5, \end{cases} \end{cases} \tag{34}$$

where  $a_{12} = \Omega_1 P_1 (1 - k_1^2 x), b_{12} = \Omega_2 P_2 k_2^2 x, c_{12} = \Omega_1 P_R (\lambda - k_R^2 y), a_{34} = \Omega_2 P_2 (1 - k_2^2 y), b_{34} = \Omega_1 P_1 k_1^2 y, c_{34} = \Omega_2 P_R (1 - \lambda - k_R^2 x), a_5 = \Omega_2 P_2 (1 - k_2^2 z), b_5 = \Omega_1 P_1 (1 - k_1^2 z), t_1 = \sigma_1^2 + \sigma_{RS_1}^2, t_2 = \sigma_2^2 + \sigma_{RS_2}^2, t_R = \sigma_R^2 + \sigma_{RS_1R}^2$ .

The above seven cases of the OP corresponds to the predefined power allocation factors as in Table 1, where

$$X = k_R^2 y + \frac{P_1 t_1 y [1 - k_2^2 y - k_1^2 (z - y)]}{P_R t_R (z - y)}, \tag{35}$$

$$Y = k_R^2 y + \frac{P_1 t_1 y (1 - k_1^2 x)}{P_R t_R x}, \tag{36}$$

$$Z = 1 - k_R^2 x - \frac{P_2 t_2 x (1 - k_2^2 y)}{P_R t_R y}, \tag{37}$$

$$T = 1 - k_R^2 x - \frac{P_2 t_2 x [1 - k_1^2 x - k_2^2 (z - x)]}{P_R t_R (z - x)}. \tag{38}$$

**Table 1** Power allocation scheme

Case	Power allocation factor $\lambda$	Outage links
1	$(k_R^2 y, \min\{X, Z\})$	$R \rightarrow S_1, S_1 \rightarrow R, S_2 \rightarrow R$
2	$(X, \min\{Y, Z\})$	$R \rightarrow S_1, S_1 \rightarrow R, S_2 \rightarrow R, R_{sum}$
3	$(Y, Z)$	$S_1 \rightarrow R, S_2 \rightarrow R, R_{sum}$
4	$\left( \begin{matrix} \max\{k_R^2 y, Z\}, \\ \min\{1 - k_R^2 x, Y\} \end{matrix} \right)$	$R \rightarrow S_1, S_1 \rightarrow R, R \rightarrow S_2, S_2 \rightarrow R, R_{sum}$
5	$\left( \begin{matrix} \max\{k_R^2 y, Z\}, \\ \min\{1 - k_R^2 x, Y\} \end{matrix} \right)$	$R \rightarrow S_1, S_1 \rightarrow R, R \rightarrow S_2, S_2 \rightarrow R$
6	$(\max\{Y, Z\}, T)$	$S_1 \rightarrow R, R \rightarrow S_2, S_2 \rightarrow R, R_{sum}$
7	$(\max\{Y, T\}, 1 - k_R^2 x)$	$S_1 \rightarrow R, R \rightarrow S_2, S_2 \rightarrow R$

*Proof* 1) When  $1 - k_1^2 x \leq 0$  or  $\lambda - k_R^2 y \leq 0$  or  $1 - \lambda - k_R^2 x \leq 0$  or  $1 - k_2^2 y \leq 0$  or  $(1 - k_1^2 z \leq 0 \& 1 - k_2^2 z \leq 0)$ , at least one of the five cases in Eqs. 23, 24, 25 always occurs, therefore OP = 1.

2) When all the above-stated conditions do not occur simultaneously, we can determine the OP as follows: let  $\mathcal{P}_{out_{12}} = \Pr\{\mathcal{A}\}$ ,  $\mathcal{P}_{out_{34}} = \Pr\{\mathcal{B}\}$ ,  $\mathcal{P}_{out_5} = \Pr\{\mathcal{C}\}$  with the events  $\mathcal{A}, \mathcal{B}, \mathcal{C}$  defined as in Eq. 27, we have

$$\mathcal{P}_{out_{12}} = \begin{cases} 1 - Q_1, \lambda \geq Y, \\ 1 - Q_2, \lambda < Y. \end{cases} \tag{39}$$

$$\mathcal{P}_{out_{34}} = \begin{cases} 1 - Q_3, \lambda \leq Z, \\ 1 - Q_4, \lambda > Z. \end{cases} \tag{40}$$

$$x \mathcal{P}_{out_5} = 1 - Q_5. \tag{41}$$

Based on these equations, we can obtain the OP of the IBFD DF-TWR system given by Eq. 29. For detailed derivation, see Appendix A.  $\square$

*Remark* To gain more insight about the system behavior, we derive the asymptotic expression of OP in the case of the transmit power is extremely large. Specifically, we consider the case that the three nodes are identical by setting  $\mathcal{R}_1 = \mathcal{R}_2 = \mathcal{R}, k_1 = k_2 = k_R = k, \Omega_1 = \Omega_2 = \Omega, \sigma_{RSI_1}^2 = \sigma_{RSI_2}^2 = \sigma_{RSI_R}^2 = \sigma_{RSI}^2, \sigma_1^2 = \sigma_2^2 = \sigma_R^2 = \sigma^2, P_1 = P_R = P_2 = P, \tilde{\Omega}_1 = \tilde{\Omega}_2 = \tilde{\Omega}_R = \tilde{\Omega}$ , and  $\lambda = 0.5$ . These settings lead to  $x = y, a_{12} = a_{34} = \Omega P(1 - k^2 x), b_{12} = b_{34} = \Omega P k^2 x, c_{12} = c_{34} = \Omega P(0.5 - k^2 x), a_5 = b_5 = \Omega P(1 - k^2 z), t_1 = t_2 = t_R = t = \sigma^2 + \tilde{\Omega} P$ . In addition, applying approximation of the exponent functions, i.e.  $\exp(-x) \approx 1 - x$  and  $\exp(x) \approx 1 + x$  when  $x \rightarrow 0$ , we can calculate the values of  $Q_1, Q_2, Q_3, Q_4$ , and  $Q_5$  as follows

$$Q_1 \approx \frac{a_{12}}{a_{12} + b_{12}} \left( 1 - \frac{x t_R}{a_{12}} \right) = (1 - k^2 x) \left( 1 - \frac{x t}{\Omega P(1 - k^2 x)} \right), \tag{42}$$

$$Q_2 \approx \left( 1 - \frac{y t_1}{c_{12}} \right) \left[ 1 - \frac{b_{12}}{a_{12} + b_{12}} \left( 1 + \frac{x t_R c_{12} - y t_1 a_{12}}{b_{12} c_{12}} \right) \right] = \left( 1 - \frac{x t}{\Omega P(0.5 - k^2 x)} \right) \left( 1 - k^2 x + \frac{0.5 x t}{\Omega P(0.5 - k^2 x)} \right), \tag{43}$$

$$Q_3 \approx \frac{a_{34}}{a_{34} + b_{34}} \left( 1 - \frac{y t_R}{a_{34}} \right) = (1 - k^2 x) \left( 1 - \frac{x t}{\Omega P(1 - k^2 x)} \right), \tag{44}$$

$$Q_4 \approx \left( 1 - \frac{x t_2}{c_{34}} \right) \left[ 1 - \frac{b_{34}}{a_{34} + b_{34}} \left( 1 + \frac{y t_R c_{34} - x t_2 a_{34}}{b_{34} c_{34}} \right) \right] = \left( 1 - \frac{x t}{\Omega P(0.5 - k^2 x)} \right) \left( 1 - k^2 x + \frac{0.5 x t}{\Omega P(0.5 - k^2 x)} \right), \tag{45}$$

$$Q_5 \approx \left( 1 + \frac{z t_R}{a_5} \right) \left( 1 - \frac{z t_R}{a_5} \right) = \left( 1 + \frac{z t}{\Omega P(1 - k^2 z)} \right) \left( 1 - \frac{z t}{\Omega P(1 - k^2 z)} \right). \tag{46}$$

In the case the transmit power is extremely large, i.e.  $P \rightarrow \infty$ , we have

$$\lim_{P \rightarrow \infty} Q_1 = \lim_{P \rightarrow \infty} Q_3 = (1 - k^2 x) \left( 1 - \frac{\tilde{\Omega} x}{\Omega(1 - k^2 x)} \right), \tag{47}$$

$$\lim_{P \rightarrow \infty} Q_2 = \lim_{P \rightarrow \infty} Q_4 = \left( 1 - \frac{\tilde{\Omega} x}{\Omega(0.5 - k^2 x)} \right) \left( 1 - k^2 x + \frac{0.5 \tilde{\Omega} x}{\Omega(0.5 - k^2 x)} \right), \tag{48}$$

$$\lim_{P \rightarrow \infty} Q_5 = \left( 1 + \frac{\tilde{\Omega} z}{\Omega(1 - k^2 z)} \right) \left( 1 - \frac{\tilde{\Omega} z}{\Omega(1 - k^2 z)} \right). \tag{49}$$

As shown in above expressions, the values of  $Q_1, Q_2, Q_3, Q_4$ , and  $Q_5$  in the high transmit power regime depend on the average channel gain ( $\Omega$ ), the SIC capability of FD device ( $\tilde{\Omega}$ ), the HI factor ( $k$ ), and the minimum required

data rate  $(x, z)$ . Since  $\Omega, \tilde{\Omega}, x, z, k$  are constants, the values of  $Q_1, Q_2, Q_3, Q_4$ , and  $Q_5$  are constants in high transmit power. Thus, the OP is a constant in the high transmit power regime. In other word, the joint and cross-impacts of hardware impairments and RSI cause OP of the IBFD DF-TWR system saturated in the high SNR regime.

### 3.2 Throughput analysis

Throughput  $\mathcal{T}$  of the system is defined as the ratio of the average number of packets successfully transmitted in a given time interval to the number of attempted transmissions [35]. The throughput of the IBFD DF-TWR system is expressed as

$$\mathcal{T} = \mathcal{R}(1 - \mathcal{P}_{\text{out}}), \tag{50}$$

where  $\mathcal{R}$  is the nominal transmission rate (bit/s/Hz) and  $\mathcal{P}_{\text{out}}$  is given in Eq. 29.

### 3.3 SEP analysis

The system SEP for a given modulation scheme is given by [9]:

$$\text{SEP} = \alpha \mathbb{E}\{Q(\sqrt{\beta\gamma})\} = \frac{\alpha}{\sqrt{2\pi}} \int_0^\infty F\left(\frac{t^2}{\beta}\right) e^{-\frac{t^2}{2}} dt, \tag{51}$$

where  $Q(x) = \frac{1}{\sqrt{2\pi}} \int_x^\infty e^{-t^2/2} dt$  is the Gaussian function;  $\gamma$  is the receive SINDR of the system;  $\alpha$  and  $\beta$  are decided by the modulation format, e.g.  $\alpha = 1, \beta = 2$  for the binary phase-shift keying (BPSK) modulation,  $\alpha = 2, \beta = 1$  for the quadrature phase-shift keying (QPSK) and 4-quadrature amplitude modulation (4-QAM) modulations [9].  $F(x)$  is the CDF of SINDR. Thus, we have  $F(x) = \mathcal{P}_{\text{out}}(x)$  which is determined using Eq. 29. If we set variable  $y$  as a function of variable  $x$  such as  $y = g(x)$  and for  $\mathcal{R}_1 = 1, \mathcal{R}_2 = 5$ , we have  $y = 31x$ . Let  $x = \frac{t^2}{\beta}$  we can obtain SEP given by

$$\text{SEP} = \frac{\alpha\sqrt{\beta}}{2\sqrt{2\pi}} \int_0^\infty \frac{e^{-\beta x/2}}{\sqrt{x}} F(x) dx. \tag{52}$$

Due to the complex expression of the OP in Eq. 29, it is not possible to simplify further the expression of the SEP in Eq. 52. However, the integration in Eq. 52 can be calculated using numerical calculation.

## 4 Optimal power allocation for the relay node

Since the system performance depends mainly on the power allocation factor  $\lambda$  of the relay node it is desired to have

it optimized. In order to achieve this objective, we propose an optimal power allocation scheme for the relay node to minimize the system OP. The objective function for the optimal  $\lambda^*$  is defined as follows

$$\lambda^* = \arg \min_{\lambda} \mathcal{P}_{\text{out}}. \tag{53}$$

**Theorem 2** *The optimal value  $\lambda^*$  for minimizing OP of the IBFD DF-TWR system with hardware impairments is determined as follows*

$$\lambda^* = \begin{cases} \min\{X, Z\}, & \text{for case 1,} \\ \min\{Y, Z\}, & \text{for case 2,} \\ (Y, Z), & \text{for case 3,} \\ \frac{(1 - k_R^2 x)\sqrt{\Omega_2 t_1 y} + k_R^2 y \sqrt{\Omega_1 t_2 x}}{\sqrt{\Omega_2 t_1 y} + \sqrt{\Omega_1 t_2 x}}, & \text{for case 4, 5} \\ \max\{Y, Z\}, & \text{for case 6,} \\ \max\{Y, T\}, & \text{for case 7,} \end{cases} \tag{54}$$

*Proof* From the exact OP expression in Eq. 29 we can find the minimal value of OP for  $\lambda = Y$  for case 1 and case 2. For case 3, since OP does not relate to  $\lambda$ , thus the value of  $\lambda$  in Table 1 is the optimal value. In case 4 and 5, since OP is a complicated function and it is not possible to find the exact value of  $\lambda$ , we resort to finding a sub-optimal value of  $\lambda$ . After some mathematical manipulations, we have  $\lambda = \frac{(1 - k_R^2 x)\sqrt{\Omega_2 t_1 y} + k_R^2 y \sqrt{\Omega_1 t_2 x}}{\sqrt{\Omega_2 t_1 y} + \sqrt{\Omega_1 t_2 x}}$ . In case 6 and case 7, the minimal value of OP is  $\lambda = Z$ . For detailed derivations of proof, see Appendix B.  $\square$

## 5 Numerical results and discussions

In this section, performances of the IBFD DF-TWR system in terms of OP and SEP are demonstrated using numerical results. In order to verify our analysis, simulation results are also provided. The impacts of both hardware impairments and RSI due to imperfect self-interference cancellation are characterized by channel response chains  $\rho_i$  with mean values of  $\Omega_i, i = 1, 2$ . The system performance under the impact of hardware impairments is compared with that of the ideal one (i.e.  $k_1 = k_2 = k_R = 0$ ) for various cases of RSI to see the degree of degradation. The effect of the power allocation on the system performance is also investigated. The system parameters used for investigation are taken from [5, 6, 20–23] and listed in Table 2 for ease of following.

Figure 2 shows the OP performance of the system versus the power allocation factor for  $P_1 = P_2 = 40$  dBm, and 4 values of  $P_R$ . The investigated threshold for the OP is set at  $\mathcal{R}_1 = \mathcal{R}_2 = 1$  bit/s/Hz, from which we obtain  $x = y = 2^1 - 1 = 1$  and  $z = x + y + xy = 3$ . The

**Table 2** Parameter settings for analyzing the system performance

Notation	Description	Fixed value	Varying range
SNR	Signal-to-noise ratio	40 dB	0 ~ 40 dB
$P_i$	Average transmit power	40 dBm	10, 20, 30, 40, 50 dBm
$\sigma_i^2$	Variance of Gaussian noise	1	None
$\sigma_{RSI_i}^2$	Variance of RSI value	1	None
$\hat{\Omega}_i$	SIC capability	-35 dB	0 ~ 0.3
$k$	HI factor	0.1	0 ~ 0.3
$\mathcal{R}$	Minimum required data rate	1 bit/s/Hz	2, 3 bit/s/Hz
$\lambda$	Power allocation factor	0.5	0 ~ 1
$(\alpha, \beta)$	Modulation pair	(1, 2)	None

aggregate level of impairments is  $k_1 = k_2 = k_R = 0.1$ . The average channel gains are  $\Omega_1 = \Omega_2 = 1$ . The RSI value is  $\sigma_{RSI_1}^2 = \sigma_{RSI_2}^2 = \sigma_{RSI_R}^2 = 1$  and the variance of AWGN is  $\sigma_1^2 = \sigma_2^2 = \sigma_R^2 = 1$ . The transmit power at the relay node is set to  $P_R = 10, 30, 40,$  and  $50$  dBm. Under this setup, the two terminal nodes play a similar role, leading to a symmetrical model which archives the best performance when the relay node allocates equal power to both sides (i.e.  $\lambda = 0.5$ ). This observation is in line with Theorem 2. For example, when  $P_R = 40$  dBm we have  $X = 0.495$ ;  $Y = 1$ ;  $Z = 0$ ;  $T = 0.495$ . Then, the value of  $\lambda$  in the Table 1 is given by (0.01, 0) for case 1; (0.495, 0) for case 2; (1, 0) for case 3; (0.01, 0.99) for cases 4 and 5; (1, 0.495) for case 6; and (1, 0.99) for case 7. Since only the range (0.01, 0.99) is suitable for  $\lambda$ , so either case 4 or case 5 occurs. Moreover, Eq. 84 becomes  $2\lambda^2 - 2\lambda + 0.9812 = 0$ . As this equation has no real root, only case 5 occurs and the optimal value of  $\lambda$  in Eq. 54 is given by  $\lambda^* = 0.5$ . It can be seen from the figure that when the relay transmit power is small, i.e.  $P_R = 10$  dBm, the impact of impairments is small

and thus performances of both the hardware impairment and ideal system are the same. However, when  $P_R$  increases, the impact of hardware impairments becomes more significant. At  $P_R = 30$  dBm, there is a significant gap between the two systems. When the relay power increases to  $P_R = 40$  dBm while the power allocation is still effective for the ideal system, it has no effect on the hardware impairment one. At higher power, i.e.  $P_R = 50$  dBm, the system OP of both the systems becomes saturated due to RSI and the power allocation is no longer effective.

Figure 3 illustrates the OP of the asymmetric system with  $P_R = 40$  dBm. The threshold, RSI, and the variance of AWGN are the same as used in Fig. 2. The transmit power and distortion factor of the two terminal nodes are set different to explore the system performance under the asymmetrical model. The figure shows that the system performs better when the power difference between the two terminal nodes is small. For example, with the distortion factor  $k_1 = k_2 = k_R = 0.1$  and the total transmit power  $P_1 + P_2 = 70$  dBm, when the power difference is small,

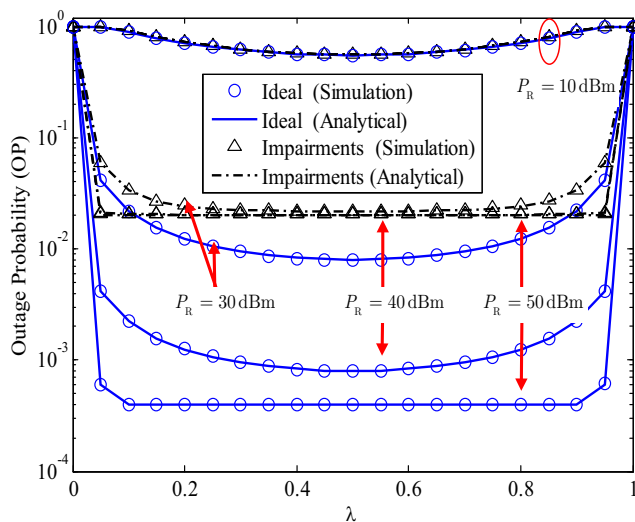


**Fig. 2** The OP performance of the symmetric FD-DF two-way relay system versus power allocation factor

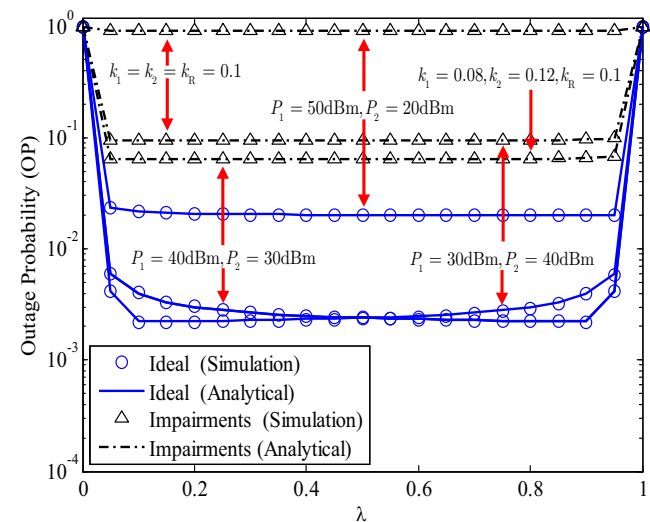


**Fig. 3** The OP performance of the asymmetric FD-DF two-way relay system versus power allocation factor

i.e.  $P_1 = 30$  dBm,  $P_2 = 40$  dBm, the OP performance is much better than the case with larger difference, i.e.  $P_1 = 50$  dBm,  $P_2 = 20$  dBm. When the evaluation parameters at the relay node are fixed and the transmit power and the distortion factor at the two terminal nodes increase, e.g.  $P_1 = 40$  dBm,  $P_2 = 30$  dBm, and  $k_1 = 0.08$ ,  $k_2 = 0.12$ , the OP performance of the system with hardware impairments exhibits a certain level of improvement. The reason is due to the fact that increasing the transmit power and decreasing the distortion factor of node  $S_1$ , and decreasing the transmit power and increasing the distortion factor at node  $S_2$  cause the hardware impairments to decrease. On the other hand, since high transmit power is used in Figs. 2 and 3, HI and RSI cause the OP of IBFD DF-TWR system to become saturated in the high SNR regime. This phenomenon is justified because  $Q_1, Q_2, Q_3, Q_4$ , and  $Q_5$  are constants (refer to Eqs. 47, 48, and 49) leading to the OP is also a constant in high transmit power.

Figure 4 plots the OP performance of the considered system versus average SNR where SNR is defined as  $SNR = \frac{P_i}{\sigma_i^2}$ ,  $i = 1, 2, R$ . Two thresholds, i.e.  $\mathcal{R}_1 = \mathcal{R}_2 = 1$  and  $\mathcal{R}_1 = \mathcal{R}_2 = 2$  bit/s/Hz are used for investigation. The HI factor is fixed at  $k_1 = k_2 = k_R = 0.1$  for small impairments. We investigate the impact of imperfect full duplexing for two cases, i.e.  $\sigma_{RSI_1}^2 = \sigma_{RSI_2}^2 = \sigma_{RSI_R}^2 = 1$  and  $\tilde{\Omega}_1 = \tilde{\Omega}_2 = \tilde{\Omega}_R = \tilde{\Omega} = -35$  dB. It is immediately realized that the performances of the perfect and impairment systems are the same at the low SNR regime, i.e. smaller than 15 dB. This means that the impact of hardware impairments can be neglected. However, for high SNR values this impact becomes profound, making the OP plots of the hardware impairment systems become saturated very soon. In the first RSI scenario ( $\sigma_{RSI_1}^2 = \sigma_{RSI_2}^2 = \sigma_{RSI_R}^2 = 1$ ), since RSI

is fixed when power of all nodes increases, the impact of RSI is higher in the low SNR regime and becomes lesser at high SNR. However, in the second RSI scenario, the impact of the RSI is stronger at high SNR due to the fact that  $\sigma_{RSI_i}^2 = \tilde{\Omega}_i P_i$  ( $i = 1, 2, R$ ) leading to the outage floor appears sooner even for the ideal hardware system. Particularly, when  $SNR > 20$  dB the OP performance of the HI system slightly increases and reaches the outage floor at  $SNR = 40$  dB. On the other hand, the outage floor of the two RSI scenarios is the same because due to significant impact of HI on the system performance. Under the considered case, the impact of HI on the OP performance is stronger than that of RSI.

Figure 5 illustrates the impact of both RSI and HI on the OP performance. The two values used for investigation are  $\lambda = 0.5$  and  $SNR = 40$  dB. The value ranges of the distortion factor  $k$  and  $\tilde{\Omega}$  are respectively given by  $k_1 = k_2 = k_R = k \in [0, 0.3]$  and  $\tilde{\Omega}_1 = \tilde{\Omega}_2 = \tilde{\Omega}_R = \tilde{\Omega} \in [0, 0.3]$ . It is noted that performance at  $k = 0$  and  $\tilde{\Omega} = 0$  corresponds to the case of the ideal hardware HD system. The figure clearly shows the strong impact of both RSI and HI on the OP of the system. Moreover, HI has more impact on the outage performance than RSI does.

Figure 6 shows the throughput characteristics of the system versus the power allocation factor  $\lambda$  for 3 typical transmission rates  $\mathcal{R} = 1, 2, 3$  bit/s/Hz. The following parameters are used for investigation:  $P_1 = P_2 = P_R = 30$  dBm,  $\sigma_{RSI_1}^2 = \sigma_{RSI_2}^2 = \sigma_{RSI_R}^2 = 1$  and  $k_1 = k_2 = k_R = 0.1$ . The figure shows that HI decreases the system throughput significantly, in particular at high transmission rates. For example, at  $\mathcal{R} = 2$  bit/s/Hz, it causes the throughput to decrease by 0.1 bit/s/Hz and the attained transmission efficiency is 90%. However, this performance

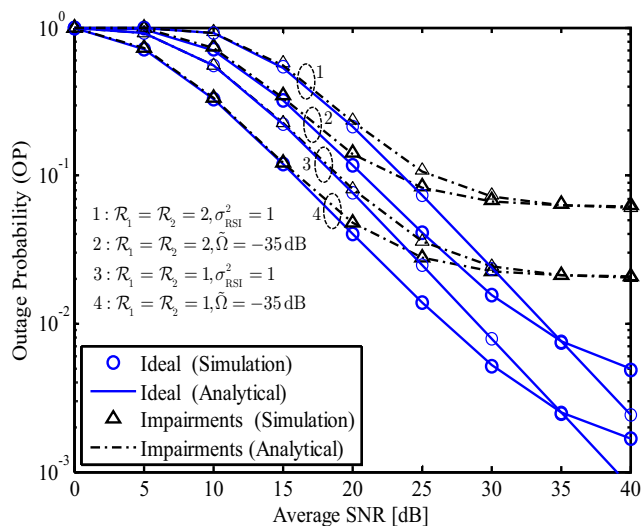


Fig. 4 The OP performance of the system versus SNR with fixed distortion factor and RSI

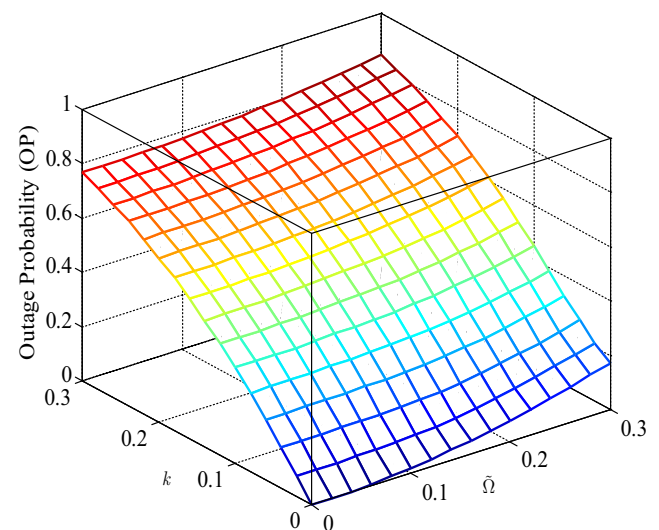
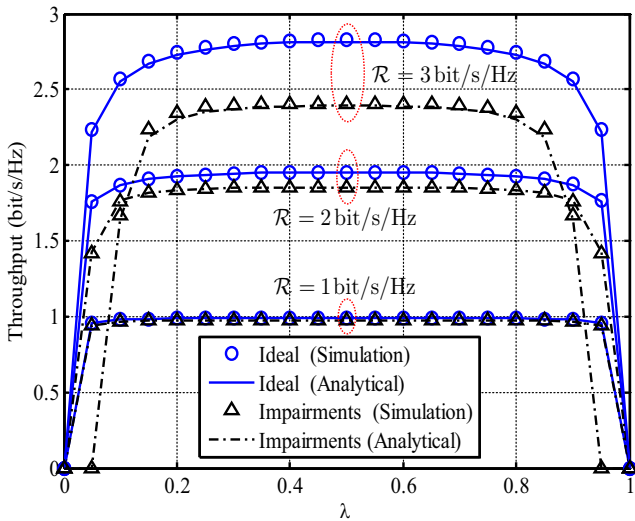


Fig. 5 The OP performance versus the distortion factor  $k$ ;  $SNR = 40$  dB



**Fig. 6** The throughput of the system versus the power allocation factor  $\lambda$  for the different  $\mathcal{R}$

loss increases to almost 0.5 bit/s/Hz leaving the system to achieve the transmission efficiency of only 80%.

Figure 7 represents the SEP performance of the considered system versus the average SNR. In this figure, the analytical curves are plotted using Eq. 52, while the marker symbols show the results obtained by Monte Carlo simulations. We set  $\tilde{\Omega}_i = -35$  dB and three levels of distortion factor as  $k = 0.08, 0.11, 0.15$ . The figure shows clearly the impact of HI on the SEP performance. For all three distortion factors, the SEP curves get saturated very early to an error floor above  $4 \times 10^{-3}$ . It can also be seen that for the HI systems, increasing the SNR to more than 25 dB does not help to attain better SEP performance.

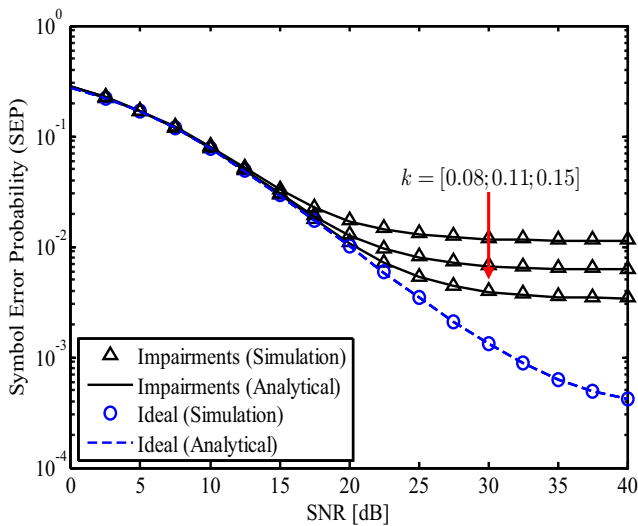


**Fig. 7** The SEP performance of the system versus the average SNR

## 6 Conclusions

In this paper, we have presented a detailed performance analysis of the IBFD decode-and-forward TWR system with transceiver impairments. Using mathematical analyses, we have derived the closed-form expressions for the three important performance measures including OP, system throughput and SEP. Performances of the system under various effects of HI and RSI were investigated using numerical calculations. It was shown that both HI and RSI have a strong impact on the system performance. Under these impacts, the system becomes saturated at high SNR regime. HI was also seen to have a stronger influence than RSI does. Although power allocation can help to improve the system performance, it is only effective for small relay transmit power such as  $P_R \leq 40$  dB. It is clear that in order to maintain an acceptable level of performance the relay needs to operate at low transmit power level. As a result, the network coverage of the IBFD decode-and-forward TWR system with HI is smaller than that with the ideal hardware and more relays are expected to be employed to attain the same communication range.

## Appendix A: Detailed derivation of Theorem 1

- 1) Consider the case when  $1 - k_1^2 x \leq 0$  or  $\lambda - k_R^2 y \leq 0$  or  $1 - \lambda - k_R^2 x \leq 0$  or  $1 - k_2^2 y \leq 0$  or  $(1 - k_1^2 z \leq 0 \& 1 - k_2^2 z \leq 0)$ , at least one of the five cases in Eq. 23, Eqs. 24, and 25 always occurs; therefore,  $\mathcal{P}_{out} = 1$ . For example, consider the probability of the first case in Eq. 23:

$$\Pr\{\gamma_{S_1R} < x\} = \Pr\left\{\frac{\rho_1 P_1}{\sigma_R^2 + \sigma_{RSIR}^2 + \rho_1 k_1^2 P_1 + \rho_2 k_2^2 P_2} < x\right\} \quad (55)$$

$$= \Pr\{\rho_1 P_1 (1 - k_1^2 x) < t_{RX} + \rho_2 P_2 k_2^2 x\}.$$

When  $1 - k_1^2 x \leq 0$ , we always have  $\rho_1 P_1 (1 - k_1^2 x) < t_{RX} + \rho_2 P_2 k_2^2 x$ . Thus,  $\Pr\{\gamma_{S_1R} < x\} = 1$ . Therefore, OP of the system is given by  $\mathcal{P}_{out} = 1$ ,

- 2) When all the conditions in 1) do not occur simultaneously,  $\mathcal{P}_{out}$  is derived as follows:

- a) When  $1 - k_1^2 x > 0$  and  $\lambda - k_R^2 y > 0$

$$\mathcal{P}_{out_{12}} = \int_0^\infty \Pr\{\rho_1 < \max(A_1, A_2)\} f_{\rho_2}(\rho_2) d\rho_2. \quad (56)$$

where

$$A_1 = \frac{t_{R^x} + \rho_2 P_2 k_2^2 x}{P_1(1 - k_1^2 x)}, A_2 = \frac{t_1 y}{P_R(\lambda - k_R^2 y)}. \tag{57}$$

To determine the  $\mathcal{P}_{out_{12}}$  from Eq. 56, we consider the case  $A_1 > A_2$ , thus

$$\frac{t_{R^x} + \rho_2 P_2 k_2^2 x}{P_1(1 - k_1^2 x)} > \frac{t_1 y}{P_R(\lambda - k_R^2 y)}. \tag{58}$$

Therefore, we have

$$\rho_2 > \frac{P_1 t_1 y (1 - k_1^2 x) - P_R t_{R^x} (\lambda - k_R^2 y)}{P_R P_2 k_2^2 x (\lambda - k_R^2 y)}. \tag{59}$$

Set

$$A_{12} = \frac{P_1 t_1 y (1 - k_1^2 x) - P_R t_{R^x} (\lambda - k_R^2 y)}{P_R P_2 k_2^2 x (\lambda - k_R^2 y)}, \tag{60}$$

if  $\rho_2 > A_{12}$ , then  $A_1 > A_2$ , otherwise we have  $A_1 \leq A_2$ . Thus, the expression (56) becomes

$$\begin{aligned} \mathcal{P}_{out_{12}} &= \int_0^{A_{12}} \Pr\{\rho_1 < A_2\} f_{\rho_2}(\rho_2) d\rho_2 \\ &+ \int_{A_{12}}^{\infty} \Pr\{\rho_1 < A_1\} f_{\rho_2}(\rho_2) d\rho_2. \end{aligned} \tag{61}$$

We now consider the condition for  $A_{12}$  to derive the closed-form expression for Eq. 61.

- If  $A_{12} \leq 0$ , then

$$\lambda \geq k_R^2 y + \frac{P_1 t_1 y (1 - k_1^2 x)}{P_R t_{R^x}} = Y. \tag{62}$$

Thus, the expression (61) becomes

$$\begin{aligned} \mathcal{P}_{out_{12}} &= \int_0^{\infty} \Pr\{\rho_1 < A_1\} f_{\rho_2}(\rho_2) d\rho_2 \\ &= 1 - Q_1. \end{aligned} \tag{63}$$

It is noted that the expression (63) is OP of the link from  $S_1$  to R.

- If  $A_{12} > 0$  then  $\lambda < Y$ .

Thus, we can calculate the two integrals in Eq. 61 numerically as follows:

$$\begin{aligned} \mathcal{P}_{out_{12}} &= \int_0^{A_{12}} \Pr\{\rho_1 < A_2\} f_{\rho_2}(\rho_2) d\rho_2 \\ &+ \int_{A_{12}}^{\infty} \Pr\{\rho_1 < A_1\} f_{\rho_2}(\rho_2) d\rho_2 = 1 - Q_2. \end{aligned} \tag{64}$$

It is noted that expression (64) is OP of the links from R to  $S_1$  and from  $S_1$  to R. This differs from the ideal hardware system. For the ideal hardware system ( $k_1 = k_2 = k_R = 0$ ) and expression (64) becomes OP of only the outage link from R to  $S_1$ .

Combining (63) with Eq. 64 we have OP of the links from  $S_1$  to R and from R to  $S_1$  as follows:

$$\mathcal{P}_{out_{12}} = \begin{cases} 1 - Q_1, & \lambda \geq Y, \\ 1 - Q_2, & \lambda < Y. \end{cases} \tag{65}$$

- b) When  $1 - \lambda - k_R^2 x > 0$  and  $1 - k_2^2 y > 0$ , using the similar method, we have

$$\mathcal{P}_{out_{34}} = \int_0^{\infty} \Pr\{\rho_2 < \max(A_3, A_4)\} f_{\rho_1}(\rho_1) d\rho_1 \tag{66}$$

where

$$A_3 = \frac{t_{R^y} + \rho_1 P_1 k_1^2 y}{P_2(1 - k_2^2 y)}, A_4 = \frac{t_2 x}{P_R(1 - \lambda - k_R^2 x)}. \tag{67}$$

Therefore, OP of the links from  $S_2$  to R and from R to  $S_2$  are defined as follows

$$\mathcal{P}_{out_{34}} = \begin{cases} 1 - Q_3, & \lambda \leq Z, \\ 1 - Q_4, & \lambda > Z. \end{cases} \tag{68}$$

When  $\lambda \leq Z$  we have  $\mathcal{P}_{out_{34}} = 1 - Q_3$  for the link from  $S_2$  to R, and when  $\lambda > Z$  we have  $\mathcal{P}_{out_{34}} = 1 - Q_4$  accounting for both the links from  $S_2$  to R and from R to  $S_2$ .

- c) When the two conditions  $1 - k_1^2 z \leq 0$  and  $1 - k_2^2 z \leq 0$  are not simultaneously satisfied, we have:

$$\mathcal{P}_{out_5} = \Pr\{C\} = \Pr\{\gamma_{sum} < z\}. \tag{69}$$

Thus

$$\mathcal{P}_{out_5} = \Pr\{\rho_1 P_1 (1 - k_1^2 z) + \rho_2 P_2 (1 - k_2^2 z) < t_{R^z}\}. \tag{70}$$

Therefore,

$$\mathcal{P}_{out_5} = 1 - Q_5. \tag{71}$$

Note that  $Q_i, i = 1 \div 5$  in Eqs. 65, 68, and 71 are defined in Eqs. 30, 31, 32, 33, and 34, respectively. Combining (65), (68), and (71), and applying the following theorem in [36]:

$$\Pr\{A \cup B \cup C\} = \Pr\{A\} + \Pr\{B\} + \Pr\{C\} - \Pr\{A \cap B\} - \Pr\{A \cap C\} - \Pr\{B \cap C\} + \Pr\{A \cap B \cap C\} \tag{72}$$

we can derive the exact expression of OP.

For example, for the outage links from  $R \rightarrow S_1$ , and from  $S_1 \rightarrow R$ , and from  $S_2 \rightarrow R$  (case 1 in Table 1), the following conditions must be simultaneously satisfied

$$\begin{cases} 1 - k_1^2 x > 0 \\ \lambda - k_R^2 y > 0 \\ 1 - \lambda - k_R^2 x > 0 \\ 1 - k_2^2 y > 0 \\ \lambda < k_R^2 y + \frac{P_1 t_1 y (1 - k_1^2 x)}{P_R t_R x} = Y \\ \lambda \leq 1 - k_R^2 x - \frac{P_2 t_2 x (1 - k_2^2 y)}{P_R t_R y} = Z \end{cases} \quad (73)$$

Therefore, the condition for power allocation factor  $\lambda$  becomes

$$\begin{cases} \lambda > k_R^2 y \\ \lambda < Y \\ \lambda \leq Z \end{cases} \quad (74)$$

where the conditions  $1 - k_1^2 x > 0$  and  $\lambda - k_R^2 y > 0$  are to guarantee that  $\mathcal{P}_{out_{12}} \neq 1$  and Eq. 65 occurs; the conditions  $1 - \lambda - k_R^2 x > 0$  and  $1 - k_2^2 y > 0$  are for  $\mathcal{P}_{out_{34}} \neq 1$  and Eq. 68 occurs; the condition

$$\lambda < k_R^2 y + \frac{P_1 t_1 y (1 - k_1^2 x)}{P_R t_R x} = Y \quad (75)$$

is the the links from  $R \rightarrow S_1$  and  $S_1 \rightarrow R$ , which is determined using Eq. 65; the condition

$$\lambda \leq 1 - k_R^2 x - \frac{P_2 t_2 x (1 - k_2^2 y)}{P_R t_R y} = Z \quad (76)$$

is for the link from  $S_2 \rightarrow R$ , which is determined using Eq. 68. When all these conditions simultaneously occur, we can determine the condition  $\mathcal{P}_{out_5} = 0$  for  $\gamma_{sum} \geq z$  (i.e. outage does not occur). Therefore, the value of power allocation factor  $\lambda$  is determined as follows

$$\rho_1 P_1 (1 - k_1^2 z) + \rho_2 P_2 (1 - k_2^2 z) \geq t_R z. \quad (77)$$

After some straightforward manipulations, we get

$$\lambda \leq k_R^2 y + \frac{P_1 t_1 y [1 - k_2^2 y - k_1^2 (z - y)]}{P_R t_R (z - y)} = X. \quad (78)$$

Combining these conditions (i.e. Eqs. 74 and 78), we have  $k_R^2 y < \lambda < \min\{X, Y, Z\}$ . Since  $X < Y$ , we have Case 1 in Table 1. When the reverse case in Eq. 78 occurs, it means  $\lambda > X$ , combining with Eq. 74, we obtain Case 2 in Table 1. Considering Case 3, the condition of  $\lambda$  for that

outage occurs in the links from  $S_1 \rightarrow R$ , and  $S_2 \rightarrow R$  is as follows

$$\begin{cases} \lambda - k_R^2 y > 0 \\ 1 - \lambda - k_R^2 x > 0 \\ \lambda \geq Y \\ \lambda \leq Z \end{cases} \quad (79)$$

Since

$$Y = k_R^2 y + \frac{P_1 t_1 y (1 - k_1^2 x)}{P_R t_R x} > k_R^2 y, \quad (80)$$

and

$$Z = 1 - k_R^2 x - \frac{P_2 t_2 x (1 - k_2^2 y)}{P_R t_R y} < 1 - k_R^2 x. \quad (81)$$

Therefore, the condition that outage occurs in the links from  $S_1 \rightarrow R$ , and  $S_2 \rightarrow R$  is determined as follows

$$Y \leq \lambda \leq Z. \quad (82)$$

Under this condition, expression (25) is always satisfied and  $\mathcal{P}_{out_5} \neq 0$ . Therefore, we have case 3. Due to this reason, we do not have scenario that outage occurs from  $S_1 \rightarrow R, S_2 \rightarrow R$  but does not occur at  $R_{sum}$ . The remaining cases can be determined by the same method. Note that since  $T > Z$  so we always have  $\max\{Y, Z, T\} = \max\{Y, T\}$  in case 7. Therefore, we have the result for this case. For case 4 and case 5, there is the same selection range  $\lambda$  but for each specific value of  $\lambda$ , only one of the two cases occurs. To have the outage links from  $R \rightarrow S_1, S_1 \rightarrow R, R \rightarrow S_2$  and  $S_2 \rightarrow R$  the condition of  $\lambda$  must be satisfied:

$$\begin{cases} \lambda - k_R^2 y > 0 \\ \lambda < Y \\ 1 - \lambda - k_R^2 x > 0 \\ \lambda > Z \end{cases} \quad (83)$$

Thus, the condition  $\max(k_R^2 y, Z) < \lambda < \min(1 - k_R^2 x, Y)$  is the value of  $\lambda$  to outage links from from  $R \rightarrow S_1, S_1 \rightarrow R, R \rightarrow S_2$  and  $S_2 \rightarrow R$ . To check the outage link at  $R_{sum}$  to choose case 4 or case 5, we need to determine the specific value of  $\lambda$ . After some transform, we get a quadratic equation, depending on the value of the roots of the quadratic equation

$$a\lambda^2 + b\lambda + c = 0 \quad (84)$$

to determine exactly case 4 or case 5, where  $a = P_R t_R z$ ,  $b = P_2 t_2 x (1 - k_2^2 z) - P_1 t_1 y (1 - k_1^2 z) - P_R t_R z (1 - k_R^2 x + k_R^2 y)$ , and  $c = P_1 t_1 y (1 - k_1^2 z) (1 - k_R^2 x) - P_2 t_2 x k_R^2 y (1 - k_2^2 z) + P_R t_R z k_R^2 y (1 - k_R^2 x)$ . If the quadratic equation has no real roots or it has exactly one real root, we have  $\mathcal{P}_{out_5} = 0$ . Combining with the condition above, we have case 5. If the quadratic equation has two distinct real roots  $\lambda_1, \lambda_2$ , with  $\lambda_1 < \lambda < \lambda_2$  then  $\mathcal{P}_{out_5} \neq 0$ . Thus, with this value of  $\lambda$  combining with the condition above, we have case 4. If

the value of  $\lambda$  changes, it means  $\lambda < \lambda_1$  or  $\lambda > \lambda_2$ , then  $\mathcal{P}_{out5} = 0$ , combining with the condition above, we have case 5.

When  $k_1 = k_2 = k_R = 0$ , this system becomes an ideal hardware system, and the expression (29) becomes expression (14) in [5] and expression (19) in [6]. Thus, Table 1 in this paper becomes the Table I in [5] and the Table III in [6].

### Appendix B

This appendix provide the detail for the optimal value of power allocation factor  $\lambda$  to minimize the OP of the system in the Theorem 2. Set  $f(\lambda) = \mathcal{P}_{out}$  and use the derivation of the  $f(\lambda)$  respect to  $\lambda$ . For conveniently, we find the derivation of the sub-function in the OP as follows

$$a'_{12} = b'_{12} = 0, a'_{34} = b'_{34} = 0, a'_5 = b'_5 = 0, c'_{12} = \Omega_1 P_R, c'_{34} = -\Omega_2 P_R,$$

$$Q'_1 = Q'_3 = Q'_5 = 0; \tag{85}$$

$$Q'_2 = \frac{\Omega_1 P_R t_1 y}{c_{12}^2} \exp\left(\frac{-t_1 y}{c_{12}}\right) \left[1 - \exp\left(\frac{x t_R c_{12} - y t_1 a_{12}}{b_{12} c_{12}}\right)\right]; \tag{86}$$

$$Q'_4 = \frac{\Omega_2 P_R t_2 x}{c_{34}^2} \exp\left(\frac{-t_2 x}{c_{34}}\right) \left[1 - \exp\left(\frac{y t_R c_{34} - x t_2 a_{34}}{b_{34} c_{34}}\right)\right]. \tag{87}$$

In case 1, we have:

$$f'(\lambda) = -Q'_2 Q_3 - Q_2 Q'_3 = -Q'_2 Q_3. \tag{88}$$

Thus,  $f'(\lambda) = 0$  when  $1 - \exp\left(\frac{x t_R c_{12} - y t_1 a_{12}}{b_{12} c_{12}}\right) = 0$ . After some manipulations, we get  $\lambda = Y$ . When  $\lambda < Y$  lead to  $Q'_2 > 0$ , so  $f'(\lambda) < 0$ . When  $\lambda > Y$ , we have  $f'(\lambda) > 0$ . Therefore,  $\lambda = Y$  is the optimal value of  $\lambda$  to minimize the OP in case 1. Combine with the condition in the Table 1, we get case 1 in Eq. 54.

In case 2, similarly case 1, we have

$$f'(\lambda) = -Q'_2 Q_3 Q_5 - Q_2 Q'_3 Q_5 - Q_2 Q_3 Q'_5 = -Q'_2 Q_3 Q_5. \tag{89}$$

From Eq. 89, the optimal value of the power allocation factor is  $\lambda = Y$ . Combine with the condition in the Table 1, we get case 2 in Eq. 54.

In case 3, we always have  $f'(\lambda) = 0$ . So the value of  $\lambda$  in the Table 1 is the optimal value.

In case 4, we find the sub-optimal power allocation for the OP. Firstly, we rewrite the OP in case 4 as follows

$$\begin{aligned} OP &= 1 - Q_2 Q_4 Q_5 = 1 - \exp\left(-\frac{t_1 y}{c_{12}} - \frac{t_2 x}{c_{34}}\right) Q_5 \\ &\times \left[1 - \frac{b_{12}}{a_{12} + b_{12}} \exp\left(\frac{x t_R c_{12} - y t_1 a_{12}}{b_{12} c_{12}}\right)\right] \\ &\times \left[1 - \frac{b_{34}}{a_{34} + b_{34}} \exp\left(\frac{y t_R c_{34} - x t_2 a_{34}}{b_{34} c_{34}}\right)\right]. \tag{90} \end{aligned}$$

From Eq. 90, the sup-optimal for the OP is the value of  $\lambda$  to maximize  $f_4 = \exp\left(-\frac{t_1 y}{c_{12}} - \frac{t_2 x}{c_{34}}\right)$ . After some mathematical manipulation, the critical point to maximize  $f_4$  is

$$\lambda = \frac{(1 - k_R^2 x) \sqrt{\Omega_2 t_1 y} + k_R^2 y \sqrt{\Omega_1 t_2 x}}{\sqrt{\Omega_2 t_1 y} + \sqrt{\Omega_1 t_2 x}}. \tag{91}$$

In case 5, similarly, we get the value of  $\lambda$  as Eq. 91.

In case 6, we have

$$\begin{aligned} f'(\lambda) &= -Q'_1 Q_4 Q_5 - Q_1 Q'_4 Q_5 - Q_1 Q_4 Q'_5 \\ &= -Q_1 Q'_4 Q_5. \tag{92} \end{aligned}$$

Set  $f'(\lambda) = 0$  to find the optimal value of  $\lambda$ , it is the root of  $Q'_4 = 0$  we have  $1 - \exp\left(\frac{y t_R c_{34} - x t_2 a_{34}}{b_{34} c_{34}}\right) = 0$ . After some manipulations, the value  $\lambda = Z$  is the root of  $Q'_4 = 0$ . When  $\lambda < Z$  lead to  $Q'_4 > 0$ , so  $f'(\lambda) < 0$ . When  $\lambda > Z$ , we have  $f'(\lambda) > 0$ . Therefore,  $\lambda = Z$  is the optimal value of  $\lambda$  to minimize the OP in case 6. Due to the fact that,  $T > Z$ , so  $\max\{Y, Z, T\} = \max\{Y, T\}$ . Combine with the condition in the Table 1, we get case 6 in Eq. 54.

In case 7, similarly case 6, the optimal value of  $\lambda$  is  $\lambda = Z$ . Therefore, the proof is completely.

### Declarations

**Conflict of interest** The authors declare no competing interests.

### References

- Ahmed I, Khammari H, Shahid A, Musa A, Kim KS, De Poorter E, Moerman I (2018) A survey on hybrid beamforming techniques in 5g: architecture and system model perspectives. *IEEE Commun Surv Tutor* 20(4):3060–3097
- Wei Z, Zhu X, Sun S, Jiang Y, Al-Tahmeesschi A, Yue M (2018) Research issues, challenges, and opportunities of wireless power transfer-aided full-duplex relay systems. *IEEE Access* 6:8870–8881
- Choi D, Lee JH (2014) Outage probability of two-way full-duplex relaying with imperfect channel state information. *IEEE Commun Lett* 18(6):933–936
- Cui H, Ma M, Song L, Jiao B (2014) Relay selection for two-way full duplex relay networks with amplify-and-forward protocol. *IEEE Trans Wirel Commun* 13(7):3768–3777

5. Li C, Wang Y, Chen Z, Yao Y, Xia B (2016) Performance analysis of the full-duplex enabled decode-and-forward two-way relay system. In: 2016 IEEE International Conference on Communications Workshops (ICC), pp 559–564
6. Li C, Chen Z, Wang Y, Yao Y, Xia B (2017) Outage analysis of the full-duplex decode-and-forward two-way relay system. *IEEE Trans Veh Technol* 66(5):4073–4086
7. Hong S, Brand J, Choi JI, Jain M, Mehlman J, Katti S, Levis P (2014) Applications of self-interference cancellation in 5G and beyond. *IEEE Commun Mag* 52(2):114–121
8. Sabharwal A, Schniter P, Guo D, Bliss DW, Rangarajan S, Wichman R (2014) In-band full-duplex wireless: challenges and opportunities. *IEEE J Sel Areas Commun* 32(9):1637–1652
9. Yang K, Cui H, Song L, Li Y (2015) Efficient full-duplex relaying with joint antenna-relay selection and self-interference suppression. *IEEE Trans Wirel Commun* 14(7):3991–4005
10. Nguyen BC, Tran XN, Tran DT, Pham XN et al (2020) Impact of hardware impairments on the outage probability and ergodic capacity of one-way and two-way full-duplex relaying systems. *IEEE Trans Veh Technol* 69(8):8555–8567
11. Xing P, Liu J, Zhai C, Wang X, Zhang X (2017) Multipair two-way full-duplex relaying with massive array and power allocation. *IEEE Trans Veh Technol* 66(10):8926–8939
12. Xia B, Li C, Jiang Q (2017) Outage performance analysis of multi-user selection for two-way full-duplex relay systems. *IEEE Commun Lett* 21(4):933–936
13. Hu J, Liu F, Liu Y (2017) Achievable rate analysis of two-way full duplex relay with joint relay and antenna selection. In: *IEEE Wireless Communications and Networking Conference (WCNC)*, pp 1–5
14. Li C, Wang H, Yao Y, Chen Z, Li X, Zhang S (2017) Outage performance of the full-duplex two-way DF relay system under imperfect CSI. *IEEE Access* 5:5425–5435
15. Li C, Xia B, Shao S, Chen Z, Tang Y (2017) Multi-user scheduling of the full-duplex enabled two-way relay systems. *IEEE Trans Wirel Commun* 16(2):1094–1106
16. Li L, Dong C, Wang L, Hanzo L (2016) Spectral-efficient bidirectional decode-and-forward relaying for full-duplex communication. *IEEE Trans Veh Technol* 65(9):7010–7020
17. Zhong B, Zhang Z (2017) Secure full-duplex two-way relaying networks with optimal relay selection. *IEEE Commun Lett* 21(5):1123–1126
18. Omri A, Behbahani AS, Eltawil AM, Hasna MO (2016) Performance analysis of full-duplex multiuser decode-and-forward relay networks with interference management. In: *IEEE Wireless Communications and Networking Conference*, pp 1–6
19. González G. J., Gregorio FH, Cousseau JE, Riihonen T, Wichman R (2017) Full-duplex amplify-and-forward relays with optimized transmission power under imperfect transceiver electronics. *EURASIP J Wirel Commun Netw* 2017(1):1–12
20. Bjornson E, Matthaiou M, Debbah M (2013) A new look at dual-hop relaying: performance limits with hardware impairments. *IEEE Trans Commun* 61(11):4512–4525
21. Bjornson E, Papadogiannis A, Matthaiou M, Debbah M (2013) On the impact of transceiver impairments on AF relaying. In: *IEEE International Conference on Acoustics, Speech and Signal Processing*, pp 4948–4952
22. Guo K, Zhang B, Huang Y, Guo D (2017) Outage analysis of multi-relay networks with hardware impairments using SECPs scheduling scheme in shadowed-Rician channel. *IEEE Access* 5:5113–5120
23. Mishra AK, Gowda SCM, Singh P (2017) Impact of hardware impairments on TWRN and OWRN AF relaying systems with imperfect channel estimates. In: *IEEE Wireless Communications and Networking Conference (WCNC)*, pp 1–6
24. Dey S, Sharma E, Budhiraja R (2019) Scaling analysis of hardware-impaired two-way full-duplex massive mimo relay. *IEEE Commun Lett* 23(7):1249–1253
25. Nguyen BC, Tran XN (2019) Performance analysis of full-duplex amplify-and-forward relay system with hardware impairments and imperfect self-interference cancellation. *Wireless Communications and Mobile Computing*, vol 2019
26. Taghizadeh O, Stanczak S, Iimori H, Abreu G (2020) Full-duplex af mimo relaying: impairments aware design and performance analysis. In: *IEEE Global Communications Conference, GLOBECOM 2020-2020*. IEEE, pp 1–6
27. Nguyen BC, Tran XN, Nguyen TTH, Tran DT (2020) On performance of full-duplex decode-and-forward relay systems with an optimal power setting under the impact of hardware impairments. *Wireless Communications and Mobile Computing*, vol 2020
28. Radhakrishnan V, Taghizadeh O, Mathar R (2021) Impairments-aware resource allocation for fd massive mimo relay networks: Sum rate and delivery-time optimization perspectives. *IEEE Transactions on Signal and Information Processing over Networks*
29. Nguyen BC, Tran XN et al (2020) On the performance of full-duplex spatial modulation mimo system with and without transmit antenna selection under imperfect hardware conditions. *IEEE Access* 8:185 218–185 231
30. Radhakrishnan V, Taghizadeh O, Mathar R (2021) Hardware impairments-aware transceiver design for multi-carrier full-duplex mimo relaying. *IEEE Transactions on Vehicular Technology*
31. Atapattu S, Fan R, Dharmawansa P, Wang G, Evans J, Tsiftsis TA (2020) Reconfigurable intelligent surface assisted two-way communications: performance analysis and optimization. *IEEE Trans Commun* 68(10):6552–6567
32. Chen G, Xiao P, Kelly JR, Li B, Tafazolli R (2017) Full-duplex wireless-powered relay in two way cooperative networks. *IEEE Access* 5:1548–1558
33. Nguyen LV, Nguyen BC, Tran XN et al (2019) Closed-form expression for the symbol error probability in full-duplex spatial modulation relay system and its application in optimal power allocation. *Sensors* 19(24):5390
34. Nguyen BC, Thang NN, Tran XN et al (2020) Impacts of imperfect channel state information, transceiver hardware, and self-interference cancellation on the performance of full-duplex mimo relay system. *Sensors* 20(6):1671
35. Goldsmith A (2005) *Wireless communications*. Cambridge University Press
36. Leon-Garcia A, Leon-Garcia A (2008) *Probability, statistics, and random processes for electrical engineering*, 3rd ed. Pearson/Prentice Hall, Upper Saddle River

**Publisher's note** Springer Nature remains neutral with regard to jurisdictional claims in published maps and institutional affiliations.